DEVELOPMENTAL BIOLOGY **203,** 382–399 (1998)
ARTICLE NO. DB989032

Functional Interactions of Genes Mediating Convergent Extension, *knypek* and *trilobite*, during the Partitioning of the Eye Primordium in Zebrafish

Florence Marlow,* Fried Zwartkruis,† Jarema Malicki,†,‡ Stephan C. F. Neuhauss,†,§ Leila Abbas,* Molly Weaver,* Wolfgang Driever,†,¶ and Lilianna Solnica-Krezel*,†,[1]

**Department of Molecular Biology, Vanderbilt University, Box 1820, Station B, Nashville, Tennessee 37235; †Cardiovascular Research Center, Massachusetts General Hospital, 149 13th Street, Charlestown, Massachusetts 01129; ‡Department of Ophthalmology, Harvard Medical School/MEEI, 243 Charles Street, Boston, Massachusetts 02114; §Max Plank Institute for Developmental Biology, Physical Biology, Spemannstrasse 35/I, Tuebingen MA, 72076 Germany; and ¶Developmental Biology, University of Freiburg, Hauptstrasse 1, Freiburg, D-79104 Germany*

Vertebrate eye development in the anterior region of the neural plate involves a series of inductive interactions dependent on the underlying prechordal plate and signals from the midline of the neural plate, including Hedgehog. The mechanisms controlling the spatiotemporal expression pattern of *hedgehog* genes are currently not understood. Cyclopia is observed in *trilobite* (*tri*) and *knypek* (*kny*) mutants with affected convergent extension of the embryonic axis during gastrulation. Here, we demonstrate that *tri* mutants show a high frequency of partial or complete cyclopia, *kny* mutants exhibit cyclopia infrequently, while kny^{m119} tri^{m209} double-mutant embryos have dramatically reduced convergent extension and are completely cyclopic. We analyzed the relationships between the convergent extension defect, the expression of *hedgehog* and prechordal plate genes, and the formation of cyclopia in kny^{m119} and tri^{m209} mutants. Our results correlate the cyclopia phenotype with the abnormal location of *hh*-expressing cells with respect to the optic primordium. We show that cyclopia in these mutants is not due to an incompetence of *tri* and *kny* cells to respond to Hedgehog signaling. Rather, it is a consequence of exceeding a critical distance (>40–50 μm) between *hedgehog*-expressing cells and the prospective eye field. We hypothesize that at this distance, midline cells are not in an appropriate position to physically separate the eye field and that HH and other signals do not reach the appropriate target cells. Furthermore, *tri* and *kny* have overlapping functions in establishing proper alignment of the anterior neural plate and midline cells expressing *shh* and *twhh* genes when the partitioning of the eye primordium takes place.

Key Words: **gastrulation; Hedgehog; midline signaling; prechordal plate; cyclopia.**

INTRODUCTION

During vertebrate development, a series of inductive interactions and morphogenetic movements leads to the formation of an embryo with defined polarity and three germ layers (Kessler and Melton, 1994). Further, inductive interactions within and between germ layers specify and pattern organ rudiments. Vertebrate eyes develop from the anterior region of the neural plate. During neurulation, the two optic vesicles evaginate on both sides of the forebrain while maintaining an attachment to the diencephalon through the optic stalks (reviewed in Saha *et al.*, 1992). Subsequently, the optic vesicles invaginate to form bilayered optic cups which will give rise to the retina and the pigment epithelium. The surface ectoderm overlaying the

[1] To whom correspondence should be addressed at current address. Fax: (615) 343-6707. E-mail: solnicl@ctrvax.vanderbilt.edu.

0012-1606/98 $25.00

optic cups will form the lens placodes (Schmitt and Dowling, 1994).

Early embryological experiments indicate that the entire anterior region of the neural plate has potential to give rise to retinal fates (Adelmann, 1936). However, during normal development retinal fates are restricted to more lateral positions. The retinal field is resolved by suppressing retina formation in the median of the field. The prechordal plate underlying the developing eye field has been implicated in the separation of the optic primordia. After experimental removal of the prechordal plate from amphibian and chick embryos (Adelmann, 1936; Li *et al.*, 1997) or in zebrafish mutants in which the prechordal plate is absent or reduced, a single retina and subsequently cyclopia develops (Schier *et al.*, 1997; Thisse *et al.*, 1994; Strähle *et al.*, 1997). In addition, fate-mapping experiments in zebrafish embryos indicate that the ventral diencephalic precursors might physically invade the eye field such that two retinas separated by midline cells are formed (Woo and Fraser, 1995; Varga and Westerfield, University of Oregon, Eugene, OR, personal communication).

Several recent studies indicate that the division of the eye field into two involves Hedgehog signaling from cells located in the midline of the developing neuroectoderm. Members of the *hedgehog* (*hh*) gene family, consisting of at least four members in the mouse, chick, and zebrafish, encode secreted signaling proteins that function in multiple patterning processes during animal embryogenesis (for review, see Hammerschmidt *et al.*, 1997). Among the above family members, *sonic hedgehog* (*shh*) expression has been found in axial mesoderm and at later stages in the ventralmost cells along the developing neural tube in all vertebrates studied (Echelard, 1993; Krauss *et al.*, 1993; Riddle, 1993; Roelink *et al.*, 1994). In zebrafish, *tiggy-winkle hedgehog* (*twhh*) is detected in the ventral central nervous system (CNS) (Ekker *et al.*, 1995), while yet another member of the family, *echidna hedgehog* (*ehh*), is expressed exclusively in the notochord (Currie and Ingham, 1996). The reduction or absence of *shh* and *twhh* expression in zebrafish *cyclops* (*cyc*) (Ekker *et al.*, 1995; Krauss *et al.*, 1993; Macdonald *et al.*, 1995) and *one-eyed pinhead* (*oep*) (Schier *et al.*, 1997; Strähle *et al.*, 1997) mutants is correlated with cyclopia. Furthermore, mouse embryos homozygous for a targeted mutation in the *shh* gene are cyclopic (Chiang, 1996). Finally, holoprosencephaly in humans can result from mutations in the *shh* homologue (Belloni *et al.*, 1996; Kelly *et al.*, 1996; Lanoue *et al.*, 1997; Roessler *et al.*, 1996; Roux *et al.*, 1997).

In the zebrafish *cyc* mutants, cyclopia is correlated with ectopic expression of *pax6* in a bridge of tissue at the anterior pole of the neural keel in the position normally occupied by cells that form optic stalks. Concomitantly, expression of the *pax2* gene in this region is dramatically reduced or absent (Ekker *et al.*, 1995; Hammerschmidt *et al.*, 1996a; Hatta *et al.*, 1994; Macdonald *et al.*, 1995). The anterior-median tissue exhibiting abnormal *pax* gene expression differentiates as retina, resulting in the formation of a single cyclopic eye in the mutant embryos. Ectopic expression of *shh, twhh, Indian hedgehog* (*Ihh*), or a dominant negative form of protein kinase A leads to the reduction of *pax6* expression and to the suppression of retina and pigment epithelium. This is accompanied by increased *pax2* expression and hypertrophy of the optic stalks in both wild-type and *cyc* mutant embryos (Ekker *et al.*, 1995; Hammerschmidt *et al.*, 1996a; Macdonald *et al.*, 1995). A model has been proposed based on these results in which *Shh* or a related molecule (e.g., *Twhh* in zebrafish) inhibits *pax6* expression and retina and pigment epithelium development in the median anterior neural tube while promoting *pax2* expression and optic stalk differentiation in neighboring tissue (Macdonald *et al.*, 1995). According to this model the temporal and spatial distribution of midline signals including HH should be critical for proper eye development.

The genes and mechanisms involved in achieving the spatial distribution of *hh* gene expression in vertebrate embryos are currently not understood. During gastrulation, convergent extension movements lead to a narrowing of the embryonic body in the mediolateral direction (convergence) and its extension along the anterior–posterior (AP) axis (Keller *et al.*, 1992a; Keller, 1985, 1991; Warga and Kimmel, 1990). Convergent extension movements have been shown to be involved in the morphogenesis of the midline tissues that express *hh* genes, including notochord, prechordal mesendoderm, and floor plate in mouse and chick (Sausedo and Schoenwolf, 1993, 1994), as well as the neural plate in chick and frog (Keller *et al.*, 1992b; Schoenwolf and Alvarez, 1989; Schoenwolf and Smith, 1990). Mutations in three zebrafish loci required for normal convergent extension during gastrulation exhibit synopthalmia and cyclopia. *trilobite* (*tri*) mutants (Hammerschmidt *et al.*, 1996b; Solnica-Krezel *et al.*, 1996) exhibit synopthalmia and cyclopia, *silberblick* (*slb*) mutants (Heisenberg *et al.*, 1996; Heisenberg and Nüsslein-Volhard, 1997) are synopthalmic but not cyclopic, while *knypek* (*kny*) mutants (Solnica-Krezel *et al.*, 1996) infrequently exhibit synopthalmia. *slb* but not tri^{tc240} mutants exhibit shortening and compression of the ventral CNS midline expressing *shh* which could result in the cyclopia phenotype (Heisenberg *et al.*, 1996).

Here we analyzed the relationships between the convergent extension defect, the spatiotemporal expression pattern of *hedgehog* and prechordal plate genes, and the formation of cyclopia in *tri* and *kny* mutants. We present evidence that *tri* and *kny* loci functionally interact during eye development. Partial eye fusion was frequently observed in tri^{m209}, tri^{m747}, and tri^{m778} mutants and only rarely in kny^{m119} and kny^{b404} mutants. Double-mutant kny^{m119} tri^{m209} embryos exhibited a dramatic reduction of convergent extension and were invariantly cyclopic. tri^{m209} and kny^{m119} mutations synergistically affected the localization of *shh*- and *twhh*-expressing cells in the neural plate

midline at the beginning of somitogenesis. At a critical distance, greater than 30–50 μm, between the cells expressing *hh* genes and the anterior neural plate margin, the optic primordium failed to properly divide into two separate retinal fields. The location of the posterior prechordal plate cells expressing the *hlx1* gene did not correlate with the location of *hh*- expressing cells nor cyclopia. These studies and recent work on the interaction between *slb* and *tri* loci reveal a genetic network required for the proper alignment of cells interacting during vertebrate head development (Heisenberg and Nüsslein-Volhard, 1997) and implicate convergent extension movements in this process.

MATERIALS AND METHODS

Fish Maintenance

Fish were maintained in 1-, 2-, and 4-liter tanks with recirculating water essentially as described in Solnica-Krezel *et al.* (1994).

Zebrafish Mutant Strains

tri^{m209}, tri^{m747}, tri^{m778}, and kny^{m119} were identified during large-scale mutagenesis screening in the laboratory of W. Driever (Solnica-Krezel *et al.*, 1996). The tri^{m778} allele was identified as a low-penetrance defect. tri^{m778} homozygous mutant embryos were observed at a frequency of 4% (n = 442) and exhibited massive degeneration during day 1 postfertilization (dpf). $tri^{m778/m209}$ transheterozygous embryos were observed at a frequency of 8% (n = 2119) and were viable through 5 dpf. The frequency and segregation indicate that tri^{m778} may be a translocation allele. kny^{b404} was induced with γ-irradiation (C. Walker and C. Kimmel, Eugene, OR, personal communication). kny^{m119} tri^{m209} double-mutant lines were generated by crossing fish heterozygous for the kny^{m119} mutation of AB genetic background with fish heterozygous for the tri^{m209} mutation of AB genetic background.

Observation of Live Embryos

For phenotypic analysis of live mutant embryos, crosses were performed between fish of defined genotypes and embryos were collected in egg water as described in Solnica-Krezel *et al.* (1994). Live embryos were observed using Zeiss SV11 and STEMI 2000 dissecting microscopes, or an Axiophot microscope, and photographed using an Axiophot microscope as described in Solnica-Krezel and Driever (1994). In experiments testing the influence of temperature on mutant phenotype, crosses were performed and embryos were collected at 26–28.5°C. Embryos were transferred to either 32 or 22–23°C before the sphere stage, 4 h postfertilization (hpf). Embryos were returned to 26–28.5°C at the one-somite stage and analyzed further at 3 dpf. To quantify the penetrance and expressivity of the cyclopia phenotype, the cyclopia index (CI) index was determined as a sum of the ratio of mutants of class x (I–V) to the total number of mutants in the clutch, multiplied by the numerical value of the class ($x = 1 - 5$): [(# class I $\times$ 1/# mutants) + (# class II $\times$ 2/# mutants) + (# *tri* III $\times$ 3/# mutants) + (# *tri* IV $\times$ 4/# mutants) + (# *tri* V $\times$ 5/# mutants)] (see Fig. 1 and Results for description of phenotypic classes).

Whole-Mount in Situ Hybridization

In situ hybridization was performed essentially as described in Oxtoby and Jowett (1993), except instead of washing at 60°C, washes were done at 70°C. Antisense RNA probes were synthesized from cDNAs encoding *shh* (Krauss *et al.*, 1993), *twhh* (Ekker *et al.*, 1995), *hlx1* (Fjose *et al.*, 1988), *hgg1* (Thisse *et al.*, 1994), *pax2* (Krauss *et al.*, 1991a), *pax6* (Krauss *et al.*, 1991b), *dlx3* (Akimenko *et al.*, 1994), and *patched* (*ptc*) (Concordet *et al.*, 1996).

Morphometric Analysis of RNA Expression Patterns and Live Embryos

Embryos stained by whole-mount *in situ* hybridization were observed under a dissecting microscope to identify wild-type and mutant phenotypes. Embryos were then grouped according to phenotype and coded. Next, "blind" measurements were taken and embryos were decoded after all samples were measured. Measurements of tri^{m209} and kny^{m119} were performed only with embryos obtained from appropriate single heterozygotes. From the progeny of kny^{m119} tri^{m209} double heterozygotes only putative double mutants were identified and measured. Identified wild-type or mutant embryos were cleared in glycerol. Subsequently embryos were transferred to glycerol in chambers formed by bridging a coverslip across three layers of No. 2 coverslips and viewed with Nomarski optics using a Zeiss Axioplan microscope and a calibrated 10$\times$ objective. The objective was calibrated relative to an object of known dimensions using Metamorph software (Universal Imaging). Images of specific staining patterns were recorded using a Hamamatsu cooled CCD camera and viewed on a computer screen. Specific distances were measured with Metamorph image-analysis software. This was performed by drawing a straight line between two marked points (e.g., the anterior tip of the *shh* expression domain and the posterior edge of the *dlx3* expression domain) or by tracing along a specific embryonic structure (e.g., the length of an embryo).

mRNA Injections

Wild-type and mutant embryos were collected from natural spawnings. Embryos were dechorionated with pronase and washed extensively in embryo medium as described in *The Zebrafish Book* (Westerfield, 1996). *shh* or *twhh* mRNAs were synthesized from DNA templates using the mMessage mMachine kit (Ambion) and suspended in ddH_2O at 100–200 ng/μl. Phenol red (0.1%) was added to the RNA solution, and embryos were injected in the yolk at the two- to eight-cell stage using a pneumatic picopump (WPI) with a known volume of RNA solution. Following injection, embryos were cultured in embryo medium. Embryos were analyzed at 30 hpf and at 48 hpf when eye and pigment epithelia are fully established.

RESULTS

Mutations in trilobite Locus Lead to Partial Cyclopia

The zebrafish *tri* locus has been identified by virtue of mutations that lead to decreased convergent extension of the embryonic body during gastrulation (Hammerschmidt

TABLE 1
Incidence of Cyclopia in Convergent Extension Mutants

Genotype	Genetic background	Mutants		
		Total No.	No. cyclopia	% Cyclopic
tri^{m209}	AB	90	11	8
tri^{m209}	AB/India	1847	595	32
tri^{m747}	AB	65	2	3
tri$^{m209/m778}$	AB/WIK	148	9	6
kny^{m119}	AB	91	0	0
kny^{m119}	AB/India	197	37	19
kny$^{m119/b404}$	AB	130	0	0

et al., 1996b; Solnica-Krezel *et al.*, 1996). *tri*^{m209} and *tri*^{m747} mutants exhibit partial cyclopia with low penetrance in the AB genetic background in which the mutations were identified (Table 1) (Solnica-Krezel *et al.*, 1996). It was possible that the *tri*^{m209} and *tri*^{m747} alleles were hypomorphs and that the synopthalmia and partial cyclopia represented an intermediate phenotype rather than the complete loss of function. However, *tri*^{m778}, which segregates like a translocation allele (Materials and Methods), led to partial cyclopia with a low penetrance in *tri*$^{m778/m778}$ homozygous and *tri*$^{m209/m778}$ transheterozygous embryos. Additionally, synopthalmia and partial cyclopia are observed in γ-irradiation-induced *tri* alleles (J. Topczewski and L. Solnica-Krezel, unpublished observations). Since γ-irradiation-induced and *tri*^{m778} alleles most likely represent null mutations and failed to enhance cyclopia when in trans with *tri*^{m209}, we conclude that synopthalmia and partial cyclopia in *tri*$^{m209/m209}$ are not the consequence of a hypomorphic nature of this allele.

When *tri*^{m209} heterozygotes were crossed with wild-type fish of India background, the identified AB/India hybrid heterozygotes produced *tri* mutant embryos with a higher incidence of cyclopia (Table 1). Five distinct degrees of cyclopia phenotypes have been distinguished when eye pigmentation is fully developed (Fig. 1). *tri* mutants with different classes of cyclopia exhibited a fully penetrant convergent extension defect and were not viable. Class I mutants exhibited eye spacing comparable to wild-type embryos (Figs. 1A and 1B); class II mutants exhibited a decreased spacing between the eyes (Fig. 1C); in mutants of class III the eyes were touching (Fig. 1D); in mutants of class IV two distinct but clearly fused eyes were observed (Fig. 1E); and class V mutants were characterized by a single cyclopic eye (Fig. 1F). In clutches of embryos obtained from two separate lines of *tri*^{m209} AB/India hybrids, all five phenotypic classes were observed (Table 2). To quantify the penetrance and expressivity of the cyclopia phenotype in any clutch of *tri* mutants, we introduced a Cyclopia Index, CI (see Materials and Methods). In one line of *tri*^{m209} AB/India hybrids the CI was determined to be 2.17 ± 0.64, while in the second line investigated the CI was 2.45 ± 0.4 (Table 2).

The Cyclopia Phenotype in tri^{m209} *Mutants Is Cold Sensitive*

Zebrafish embryos develop normally, although at different rates, at temperatures between 23 and 32°C (Kimmel *et al.*, 1995). To test possible effects of temperature on the phenotype of *tri* mutants, clutches of embryos obtained from *tri*^{m209} AB/India hybrids were incubated at 23, 28.5, and 32°C. Analysis of these embryos indicated that the penetrance and expressivity of the cyclopia phenotype were exacerbated at 23°C and suppressed at 32°C (Table 2). The convergent extension phenotype was fully penetrant at all temperatures examined, as indicated by measurements of the AP length and the width of the *shh* expression domain at the level of the otic vesicles (Table 4). Therefore, the cyclopia phenotype is cold sensitive in *tri*^{m209} mutants.

knypek^{m119} *trilobite*^{m209} *Double Mutants Exhibit Complete Cyclopia and Additive Defects with Regard to Body Length*

kny^{m119} mutants exhibited a very similar phenotype to *tri* mutants at day 1 of development (Fig. 2), except cyclopia was observed less frequently in *kny*^{m119} mutants in AB or AB/India hybrid background (Table 1) (Solnica-Krezel *et al.*, 1996). Furthermore, *kny*^{m119} mutants exhibited a characteristic forked yolk extension and failed to develop the ventral fin (data not shown). Cyclopia was also rare in *kny*$^{b404/b404}$ (C. Walker and C. Kimmel, University of Oregon, Eugene, OR, personal communication), and additional γ-irradiation induced alleles (J. Topczewski and L. Solnica-Krezel, unpublished observations). Therefore, the low frequency of cyclopia in *kny*^{m119} mutants is not likely due to a hypomorphic nature of this allele.

Considering the similar phenotypes of *kny* and *tri*, a double-mutant line, *kny*^{m119} *tri*^{m209}, was generated to test for possible functional interactions between the two genes. In the progeny of *kny*^{m119}+/− *tri*^{m209}+/− double heterozygotes, single *tri* and *kny* mutants were identified based on the morphological characteristics described above, at expected frequencies (Fig. 2, Table 3). Furthermore, a distinct class of mutants was present at a frequency expected for double-mutant embryos. At 24 hpf these double-mutant embryos were characterized by a very short axis with a particularly shortened and dorsally kinked tail region (Fig. 2G). The AP body length of wild-type embryos was determined to be 2.3 ± 0.02 mm (n = 10) at this stage of development; *tri*^{m209} were ca. 0.5 mm shorter than wild type, 1.8 ± 0.03 mm (n = 10), and *kny*^{m119} mutants were ca. 0.6 mm shorter than wild type, 1.7 ± 0.05 mm (n = 5). The *kny*^{m119} *tri*^{m209} double mutants were half as long as wild type, 1.15 ± 0.03 mm (n = 5), indicating that the extension defect of the

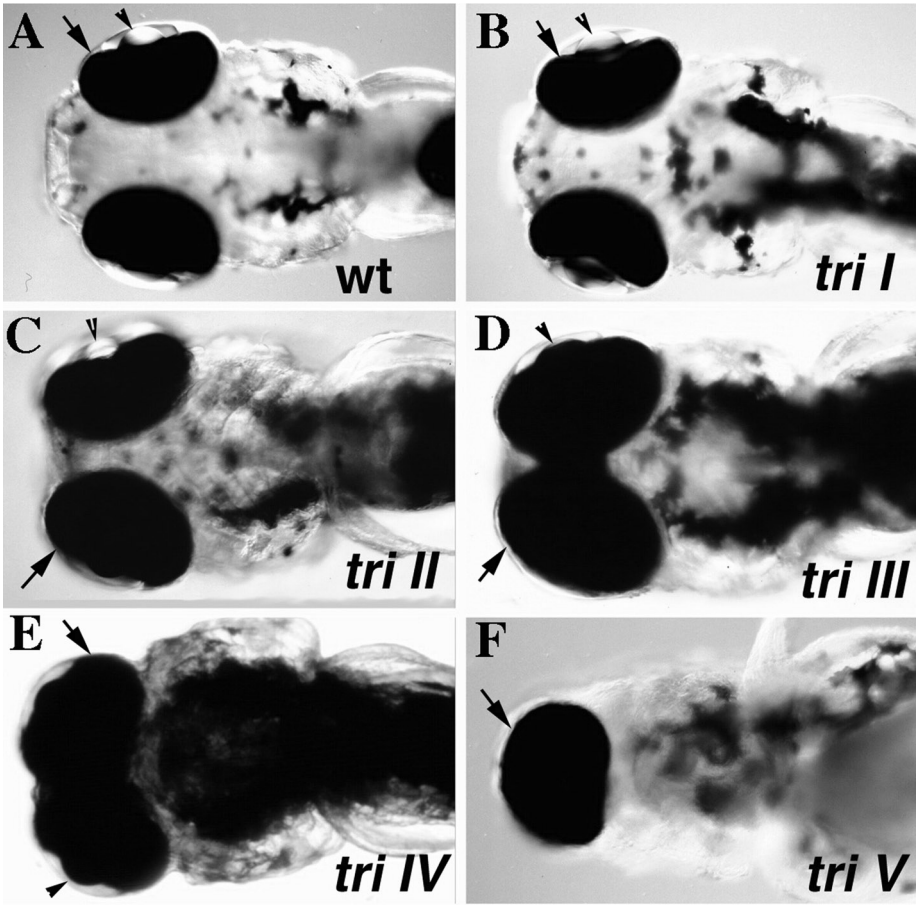

FIG. 1. Degrees of cyclopia in *tri*^{m209} mutants. Micrographs of live embryos at 3 dpf, ventral view of head region. Five classes of the cyclopia phenotype can be distinguished in *tri*^{m209} mutants. In class I mutants (B) the eye spacing is comparable to that observed in a wild-type sibling (A). In mutants of class II (C) the eye spacing is decreased. (D) In mutants of class III eyes are marginally fused. (E) The eyes are completely fused in mutants of class IV. (F) One cyclopic eye is observed in class V mutants. Retina covered by pigment epithelium (arrow).

kny^{m119} *tri*^{m209} double mutant was additive. Notably, the double mutants exhibited complete cyclopia (Fig. 2G, inset). This synergistic phenotype suggested that *tri*^{m209} and *kny*^{m119} have overlapping functions in convergent extension as well as eye development.

Interestingly, 28% of *kny*^{m119} mutants identified among the progeny of *kny*^{m119}+/− *tri*^{m209}+/− double heterozygotes exhibited partial cyclopia. This was in contrast to the lack of cyclopia observed for *kny*^{m119} mutants in AB/AB background (Table 1). It was likely that homozygous *kny*^{m119} mutant embryos exhibited cyclopia when also heterozygous for the *tri*^{m209} allele. Alternatively, another enhancer of cyclopia could be present in the *kny tri* mutant line. To distinguish between these possibilities, crosses were performed between siblings of known genotypes at the *kny* and *tri* loci, and the cyclopia index was determined in the resulting progeny (see Materials and Methods). As expected, embryos homozygous for *kny*^{m119} mutant alleles with two wild-type alleles at the *tri* locus rarely exhibited cyclopia (CI = 1.01 ± 0.01; n = 200). *kny* mutants from crosses of *kny*^{m119} *tri*^{m209} double heterozygotes with *kny*^{m119} heterozygotes had a significantly higher cyclopia index, 1.54 ± 0.32 (n= 1009). However, among these *kny* mutants only half should contain one *tri*^{m209} allele. Therefore, the estimated cyclopia index for embryos of the *kny*^{m119}−/− *tri*^{m209}−/+ genotype is 2.0 ± 0.7, considering that *kny* mutants with two wild-type alleles at the *tri* locus do not exhibit cyclopia (see above). Since less than 50% of *kny*^{m119} mutants exhibited cyclopia, these observations support the notion of *tri*^{m209} being a dominant enhancer of cyclopia in *kny*^{m119} −/− mutants. As expected from earlier experiments, double-mutant embryos obtained from these crosses exhibited complete cyclopia (CI = 4.9 ± 0.16; n = 277).

TABLE 2
Temperature Effect on the *tri*^{m209} Cyclopia Phenotype

Parental genotype	Temperature (°C)	Total No. progeny	Total No. mutants (% total)	Frequency of mutant embryos with different degree of cyclopia (%)					Cyclopia index ± SD
				Class I	Class II	Class III	Class IV	Class V	
Line #1 *tri*^{m209}	23	1354	335 (25%)	27.2	10.4	10.1	50.4	1.5	2.76 ± 0.63
AB/India	28.5	8160	1947 (24%)	57.2	5.6	7.4	29.4	0.4	2.17 ± 0.62
	32	1300	322 (25%)	94.4	2.5	1.9	1.2	0	1.09 ± 0.14
Line #2 *tri*^{m209}	23	476	134 (28%)	8.2	11.9	44.8	33.6	1.5	3.10 ± 0.40
AB/India	28.5	298	73 (25%)	26	21.9	34.2	15.1	2.7	2.45 ± 0.40
	32	625	184 (29%)	77.2	15.8	5.4	1.6	0	1.28 ± 0.26

The Cyclopia Phenotype Is Correlated with an Abnormal Distribution of shh and twhh Transcripts in Mutant Embryos

The cyclopia phenotype is often accompanied by and most likely results from the reduction or absence of *hh* gene expression in the midline of the developing neural plate (Ekker *et al.*, 1995; Krauss *et al.*, 1993; Macdonald *et al.*, 1995; Schier *et al.*, 1997; Strähle *et al.*, 1997; Chiang *et al.*, 1996). Therefore, the degree of cyclopia could reflect the abnormal expression of *shh* and possibly *twhh*. Indeed, a shortened *shh* expression domain in the AP axis has been observed in *slb*^{tx226} cyclopic mutants at the onset of somitogenesis (Heisenberg and Nüsslein-Volhard, 1997). Therefore, we analyzed the expression of *shh* and *twhh* genes in *tri*^{m209} mutants at permissive and restrictive temperatures, as well as in *kny*^{m119} and *kny*^{m119} *tri*^{m209} double-mutant embryos at the beginning of somitogenesis. *In situ* hybridization analysis indicated that at tail bud stage the expression domain of *shh* and *twhh* genes was shorter along the AP axis and broader along the mediolateral axis for both *kny*^{m119} (Figs. 3B and 3F) and *tri*^{m209} (Figs. 3C and 3G) mutants (also data not shown). This phenotype was exacerbated in putative double-mutant embryos (Figs. 3D and 3H). The abnormal shape of *shh* and *twhh* expression domains was consistent with a general convergent extension defect in the mutant embryos and likely resulted from reduced convergent extension of cells specified to express *hh* genes. Notably, the AP *shh* expression domain length appeared shorter in *kny*^{m119} mutants than in *tri*^{m209} mutants; however, cyclopia was infrequently observed for *kny*^{m119} (Figs. 3B and 3F vs Figs. 3C and 3G). This indicated that the AP shortening of the *shh* expression domain at the onset of somitogenesis was not sufficient for the cyclopia phenotype.

At 24 hpf, the overall AP length of the *shh* expression domain was shortened to a similar degree in both *tri*^{m209} (Fig. 4C) and *kny*^{m119} mutants (Fig. 4B). In contrast, while the rostral brain *shh* expression domain was normal in *kny*^{m119} mutants compared to wild type (Figs. 4A and 4B), in *tri*^{m209} mutants this expression domain was shortened (Solnica-Krezel *et al.*, 1996) and was drastically compressed in *kny*^{m119} *tri*^{m209} double mutants (Figs. 4D and 4H). In *tri*^{m209} (Fig. 4G) and *kny*^{m119} *tri*^{m209} (Fig. 4H) cyclopic mutant embryos, the forebrain expression domain appears to be posteriorly shifted with respect to the eyes. Therefore, the compression of the anterior portion, but not the overall AP length of the *shh* expression domain at 24 hpf, correlated with the cyclopia phenotype.

These observations suggested that cyclopia could be due to the abnormal location of *shh*-expressing cells with respect to the prospective eye field. To investigate this possibility, clutches of mutant embryos at the one-somite stage were hybridized simultaneously with *shh* and *dlx3* probes. *dlx3* transcripts are detected in a baseball-stitch band positioned around the edge of the prospective neural plate (Akimenko *et al.*, 1994). In wild-type embryos *shh* and *twhh* midline expression domains extended anteriorly to the posterior edge of the *dlx3* domain (Fig. 5A and data not shown). In contrast, a small gap between *shh* and *dlx3* expression domains was observed for *kny*^{m119} mutants (Fig. 5B), and an apparently larger gap was observed for *tri*^{m209} (Fig. 5C) and *kny*^{m119} *tri*^{m209} mutant embryos (Fig. 5D). This observation prompted us to measure the distance between the anterior edge of *shh* and *dlx3* domains with a digital camera and Metamorph software (see Materials and Methods). These studies revealed a correlation between the size of the gap between the *shh* and *dlx3* expression domains in the anterior neural plate and the cyclopia phenotype (Fig. 6 and Tables 1 and 2). In wild-type embryos the average *shh–dlx3* distance was smaller than 5 μm (n = 69). In *kny*^{m119} mutants, in which cyclopia was only occasionally observed, this distance was significantly larger, approximately 20 ± 11 μm (n = 17). In *tri*^{m209} embryos that developed at a permissive temperature, which suppressed cyclopia (CI = 1.1–1.3), the *shh–dlx3* distance was greater, 30 ± 15 μm (n = 15). Notably, in *tri*^{m209}

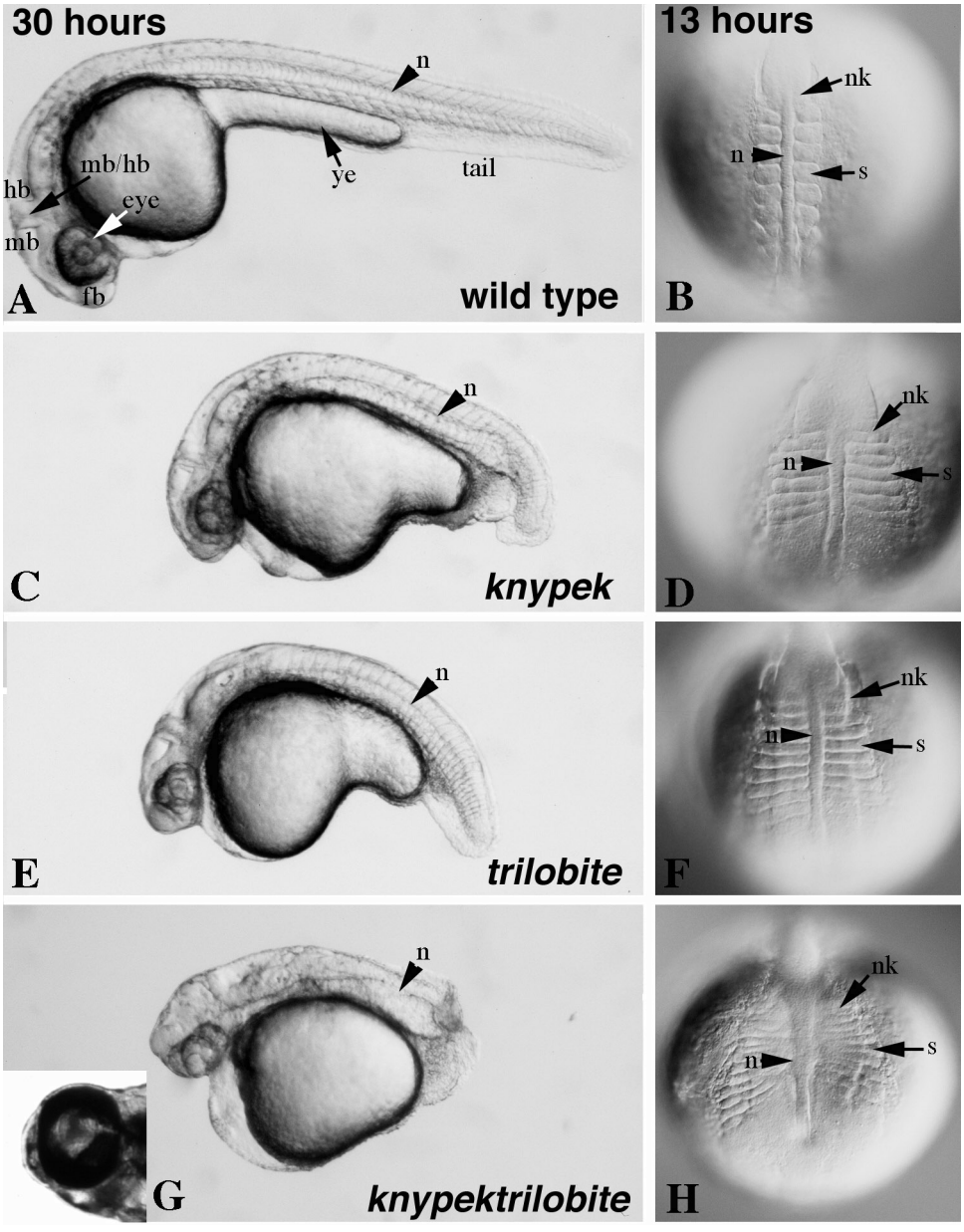

FIG. 2. *kny*^{m119} *tri*^{m209} double-mutant embryos exhibit additive defects in convergent extension during somitogenesis and 1 dpf, and a synergistic cyclopia defect, compared to single mutants. (A, C, E, G) Dissecting microscope images, lateral view of live embryos at 30 hpf. The length of the embryo is decreased in *kny*^{m119} (C) and *tri*^{m209} (E) mutants and dramatically decreased in the double mutant (G) compared to wild type (A). Abnormal shape of the yolk cell and cyclopia are seen in the double mutant (G, inset). (B, D, F, H) Dorsal views of live embryos at 13 hpf using Nomarski optics. The mediolateral width and AP extension of somites (s), notochord (n), and neural keel (nk) are affected in an additive fashion in double mutants (H) compared to *kny*^{m119} (D) and *tri*^{m209} (F) single-mutant embryos. fb, forebrain; hb, hindbrain; mb, midbrain; mb/hb, midbrain–hindrain boundary; ye, yolk extension.

embryos which developed at the restrictive temperature which leads to a high incidence of cyclopia (CI = 2.8–3.1), the average *shh–dlx3* distance was markedly increased to 50 ± 22 μm (n = 9). Finally, the *shh–dlx3* distance was extremely large, ca. 90 ± 27 μm (n = 12), in cyclopic *kny*^{m119} *tri*^{m209} double-mutant embryos (CI = 5). The dimension of the *shh–dlx3* gap in *kny*^{m119} *tri*^{m209} double mutants was larger than the sum of the gaps observed for

TABLE 3
Phenotypic Classes Observed in Progeny of *m119 +/− m209 +/− × m119 +/− m209+/−*

Phenotype	No. observed	No. expected	$(O - E)^2/E$	No. with cyclopia	% with cyclopia
Wild type	2549	2539	0.039	0	0
trilobite	840	848	0.075	649	77.3
knypek	844	848	0.019	286	33.9
knypek trilobite	277	275	0.015	277	100
Total	4510	4510			

The observed numbers of wild-type and single- and double-mutant embryos are not significantly different from those expected for two independently segregating genes. $\chi^2 = 0.148$, $P > 0.975$.

the single mutants (Fig. 6). Therefore, there was a synergistic interaction between the two mutations with respect to the size of the *shh–dlx3* gap, as there was for the cyclopia phenotype. Based on these results we hypothesized that excessive distance between the *hh*-expressing cells and the anterior neural plate (>40–50 μm) resulted in failure to partition the optic primordium and led to synopthalmia or cyclopia.

The measurements of the AP dimension of the embryo (the length of the embryo from the anterior tip of the forming polster to the tail bud) confirmed that there was no simple relationship between the degree of the overall convergent extension defect and cyclopia (Table 4). The double mutants exhibited the shortest axis and the largest *shh–dlx3* gap (Table 4). However, the AP length defect with respect to wild-type embryos was ca. 100 μm larger in kny^{m119} than tri^{m209} mutants (Table 4). The convergence defect was further examined by measuring the width of the

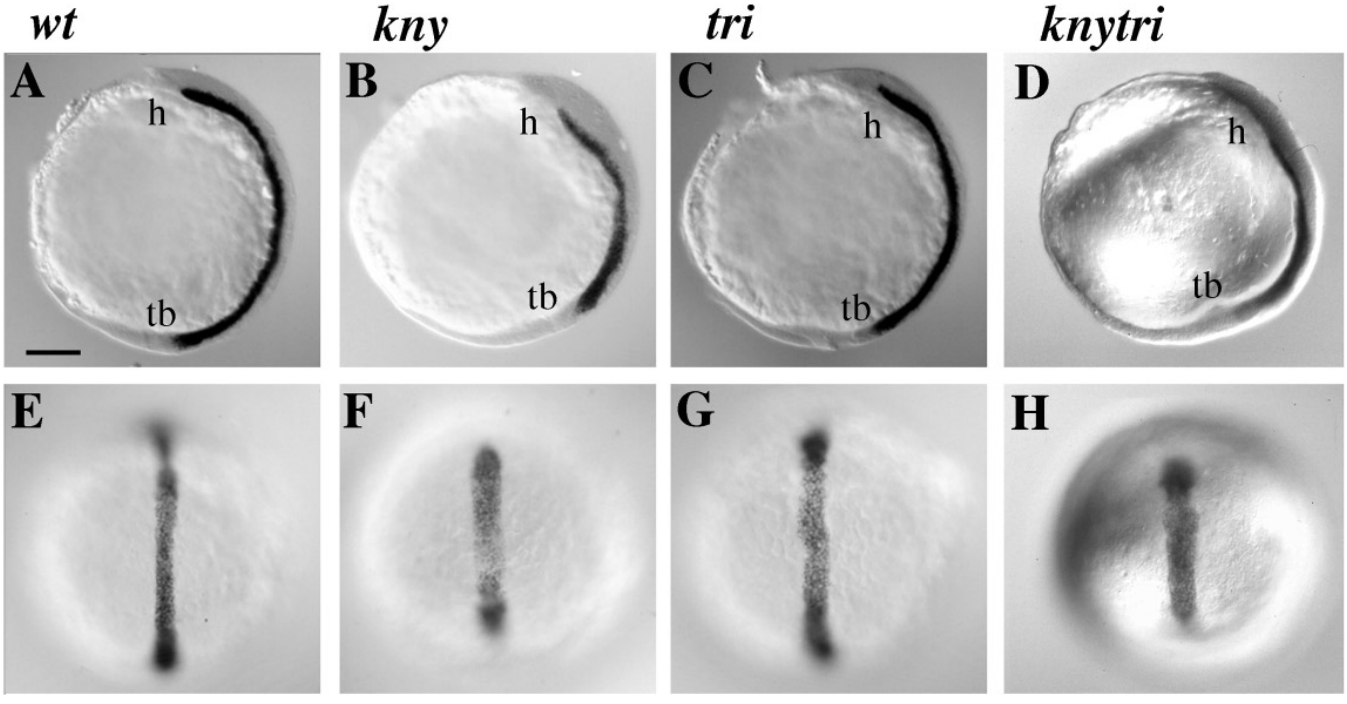

FIG. 3. Comparative expression of *shh* in wild-type (A, E), tri^{m209} (C, G), kny^{m119} (B, F), and *kny tri* (D, H) embryos at bud stage (10.5 hpf). The *shh* expression domain is shortened in the AP direction and broadened in the mediolateral direction; this phenotype is more pronounced in kny^{m119} (B, F) and kny^{m119} tri^{m209} (D, H) than in tri^{m209} (C, G) embryos. (A–D) Lateral views, dorsal to the right and anterior at the top; (E–H) dorsal views, anterior toward the top. Tailbud (tb), prospective head region (h). Bar, 120 μm.

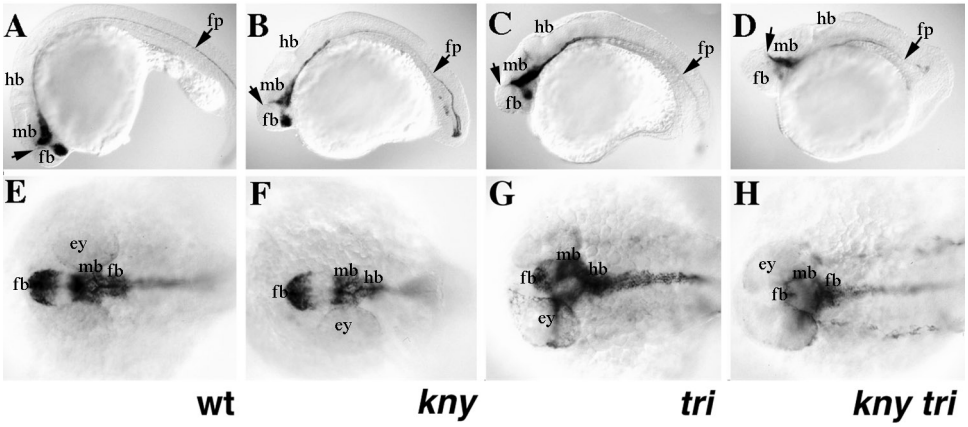

FIG. 4. Abnormal expression of *shh* gene at 30 hpf is correlated with the cyclopia phenotype in tri^{m209} and kny^{m119} tri^{m209} mutant embryos. (A–D) Lateral views. *shh* expression in wild-type (A) and kny^{m119} mutants (B) extends to the anterior tip of the embryo. In contrast, the *shh* expression domain is compressed along the AP axis and fails to extend to the anterior tip of the embryo in cyclopic tri^{m209} (C) and kny^{m119} tri^{m209} (D) mutants. The telencephalon occupies a more dorsal location in tri^{m209} (C) and kny^{m119} tri^{m209} (D) embryos than observed for wild-type embryos (A). (E–H) Dorsal views. *shh* expression in the hypothalamus is compressed and positioned more posteriorly in tri^{m209} (G) and kny^{m119} tri^{m209} (H) mutant embryos compared to wild-type (E) and kny^{m119} (F) embryos. Arrows, middiencephalic boundary; mb, midbrain; ey, eye; hb, hindbrain; fb, forebrain; fp, floor plate expression in the spinal cord.

shh expression domain and the width of the neural plate at the level of the otic placodes marked by stronger expression of the *dlx3* gene (Akimenko *et al.*, 1994). The measurements revealed similar defects for kny^{m119} and tri^{m209} mutants compared to their wild-type siblings. However, the convergence defect in double mutants appeared additive.

Prechordal Plate and hh Expression

Cyclopia is often correlated with a lack or reduction of prechordal mesendoderm (Ekker *et al.*, 1995; Macdonald and Wilson, 1996; Schier *et al.*, 1997; Strähle *et al.*, 1997). Inappropriate location of the prechordal mesendoderm could result in the abnormal positioning of *hh*- expressing cells in the overlying neuroectoderm. During late gastrulation, expression of *hlx1* homeobox gene is detected in the posterior prechordal region of the hypoblast (Fjose *et al.*, 1994), while *hgg1* is expressed in the anterior-most prechordal plate (polster) (Thisse *et al.*, 1994). Prechordal plate is present, and the *hlx1* expression domain is shorter in kny^{m119} and tri^{m209} mutants (Solnica-Krezel *et al.*, 1996). To address whether the prechordal plate determines the position of *hh* expression, we examined *hlx1, pax2, dlx3,* and *hgg*1 RNA expression in tri^{m209}, kny^{m119}, and kny^{m119} tri^{m209} double mutants by simultaneous *in situ* hybridization.

Examination of *hgg1* and *dlx3* revealed that the polster was positioned anterior to the neural plate in wild-type (Fig. 5I) and tri^{m209} (Fig. 5K) embryos. However, in kny^{m119} (Fig. 5J), the polster was abnormally localized beneath the neural plate, as was reported for slb^{tx226} mutant embryos (Heisenberg and Nüsslein-Volhard, 1997), and was partially underlying the neural plate in kny^{m119} tri^{m209} double-mutant embryos (Fig. 5L). There was no simple correlation between *hgg1* position and cyclopia, as kny^{m119} embryos were most affected.

Furthermore, this analysis indicated that a gap existed between the *hlx1* and *dlx3* expression domains for all genotypes analyzed (Figs. 5I–5L). To determine if the distance between *hlx1*-expressing cells and the anterior edge of the neural plate correlated with cyclopia and *shh* expression, measurements were taken with Metamorph software as described previously. The *hlx-dlx3* gap was 6.0 ± 6.9 μm (n = 40) for wild type, 35.1 ± 13.9 μm (n = 10) for tri^{m209}, 40.9 ± 15.5 μm (n = 10) for kny^{m119}, and 45.2 ± 7.0 μm (n = 10) for kny^{m119} tri^{m209} embryos. Next, we compared distance changes between *dlx*3 and *hlx*1, as well as between *dlx3* and *shh*, at temperatures that suppressed and enhanced cyclopia in tri^{m209} mutants. The *shh–dlx3* results were consistent with those described previously in this paper (Fig. 6). These studies revealed no correlation between the position of *hlx1* and *shh* expression at this stage of development. Specifically, at the permissive temperature (32°C), the *hlx1–dlx3* gap was larger compared to the normal developmental temperature. This was opposite to the *hh–dlx3* gap, which was reduced at the permissive relative to normal developmental temperature. Therefore, it is not likely that the location of the *hh*-expressing cells at this stage of development is determined by the position of the *hlx1*-expressing cells within the prechordal mesendoderm.

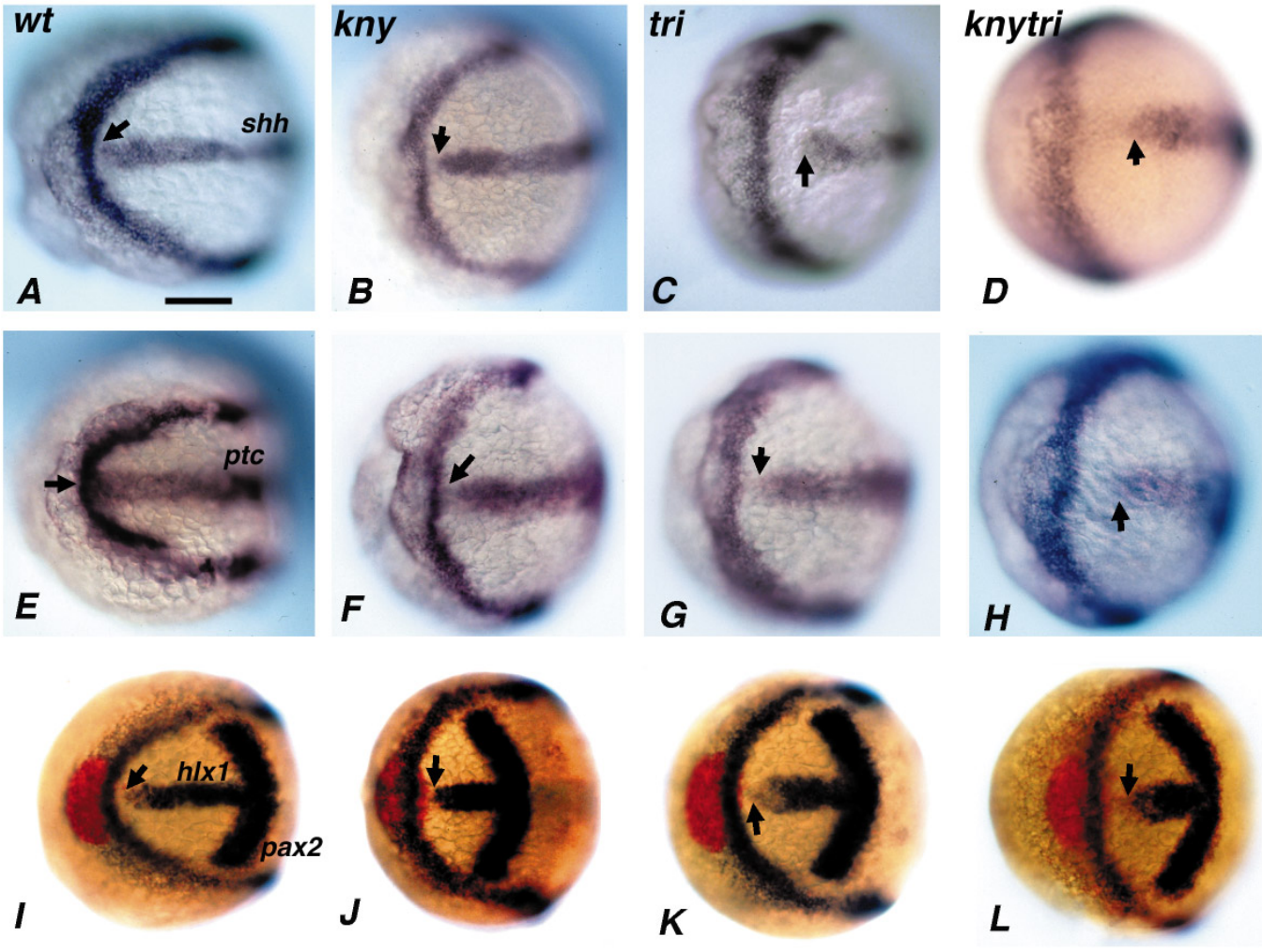

FIG. 5. Comparative expression of *shh* (A–D), *ptc* (E–H), and prechordal plate markers *hgg1* and *hlx1* (I–L) relative to *dlx3*, baseball-stitch band around the anterior edge of the neural plate in wild-type (A, E, I), kny^{m119} (B, F, J), tri^{m209} (C, G K), and kny^{m119} tri^{m209} (D, H, L) visualized by *in situ* hybridization. The *shh* expression domain in kny^{m119} (B), tri^{m209} (C), and kny^{m119} tri^{m209} (D) is localized abnormally with respect to the anterior edge of the neural plate at the one-somite stage. This abnormal localization is also observed for *ptc1* expression. A gap is observed between *ptc1* and *dlx3* for tri^{m209} (G) and kny^{m119} tri^{m209} (H) mutant embryos, but not for wild-type (E) or kny^{m119} (F) embryos. In addition, a gap is observed between *hlx1* and *dlx3* for all embryos including wild type (I–L). *hgg1* (red) is positioned anterior to the neural plate in wild-type (I), tri^{m209} (K), and kny^{m119} tri^{m209} (L) embryos and underlies the neural plate in kny^{m119} embryos (J). Arrows indicate the anterior extent of *shh* (A–D), *ptc* (E–H), or *hlx1* (I–L) expression. Bar, 60 μm.

Cyclopic kny^{m119} tri^{m209} Mutants Have Altered pax2 and pax6 Expression Patterns

Lack of HH signaling in *cyc* mutants leads to ectopic expression of the *pax6* gene in the median region of the anterior neural plate and to a reduction or absence of the *pax2* gene expression (Ekker *et al.*, 1995; Hammerschmidt *et al.*, 1996a; Macdonald *et al.*, 1995). Failure of HH signaling to reach the anterior region of the neural plate would be expected to produce similar changes in *pax* gene expression in convergent extension mutants. In wild-type embryos at 24 hpf, *pax6* RNA was detected in two separate domains and was absent from the anteriormost region of neuroectoderm (Fig. 7C). However, in kny^{m119} tri^{m209} mutants *pax6* RNA was uniformly distributed throughout the anterior neural keel including the median region normally devoid of *pax6* expression (Fig. 7D). In contrast to the two distinct domains observed in wild-type siblings (Fig. 7E), *pax2* RNA was expressed in a single domain centered at the midline in the kny^{m119} tri^{m209} double mutants (Fig. 7F). Therefore, a

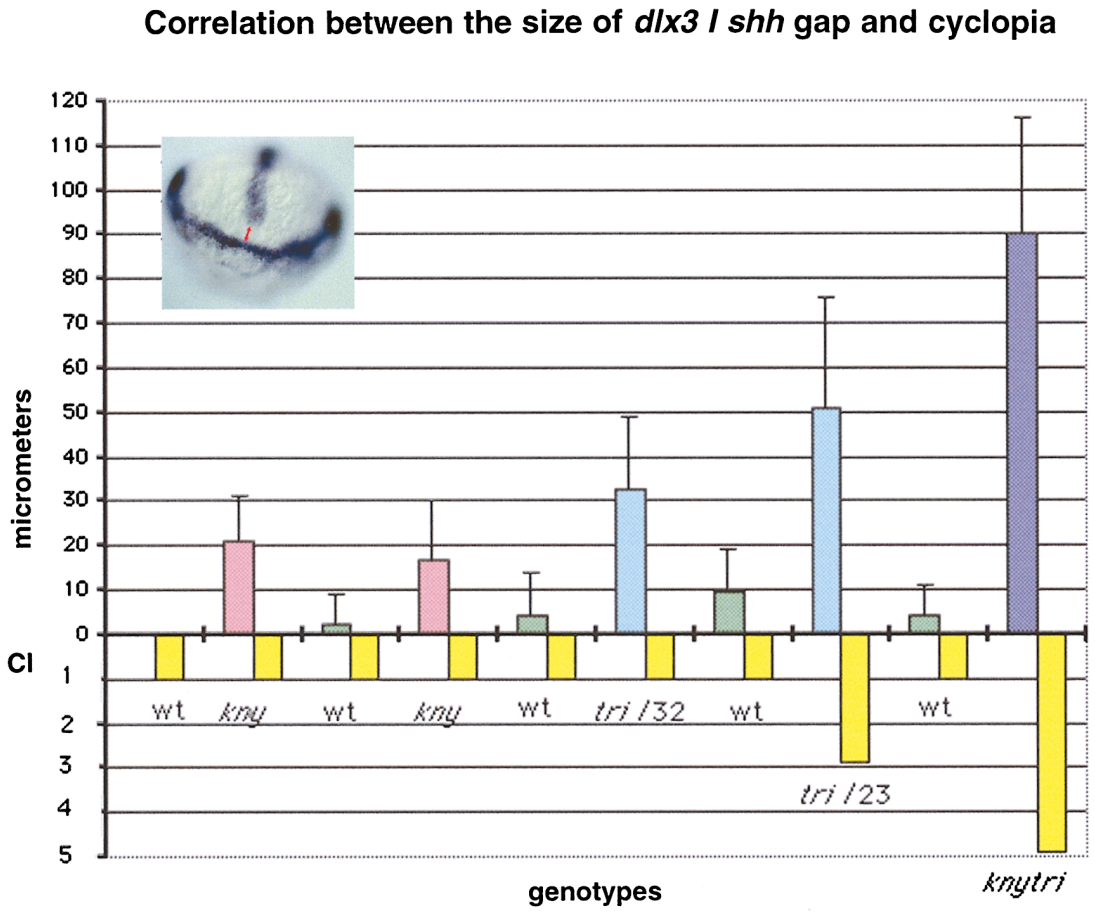

FIG. 6. The *shh–dlx3* gap dimensions correlate with the cyclopia phenotype in convergent extension mutants. The dimensions of the *shh–dlx3* gap were measured as described under Materials and Methods. Expression was visualized by whole-mount *in situ* hybridization. The graph shows dimensions in micrometers of the *shh–dlx3* gap (above the *x* axis) and their corresponding CI (below the *x* axis) for mutants and their wild-type siblings (see Materials and Methods for calculation of CI). Two independent samples of kny^{m119} at the permissive temperature are shown, as well as one sample of tri^{m209} mutant siblings incubated at permissive temperature (32°C) or restrictive temperature (23°C), and a kny^{m119} tri^{m209} double-mutant sample. Error bars show standard deviations for each sample.

failure to partition the optic primordium leads to cyclopia in these mutants.

Mutant Embryos Can Respond to Hedgehog Signaling

Another plausible explanation for the cyclopia phenotype and the abnormalities in *pax2* and *pax6* gene expression described above is that *tri* and *kny* have partially redundant functions required in the neuroectoderm for HH signal reception. To test this possibility synthetic mRNAs encoding *shh* and *twhh* were injected into one- to eight-cell-stage embryos of wild-type, tri^{m209}, kny^{m119}, and kny^{m119} tri^{m209} genotypes. Ectopic expression of *hh* was confirmed by *in situ* hybridization. Ectopic expression of *ptc* in response to ectopic *hh* was observed, as reported by Concordet, indicating that the injected mRNA was functional (data not shown and Concordet *et al.*, 1996). Consistent with earlier reports, the prominent phenotypes were unilateral and bilateral reduction of retina and pigment epithelium in wild-type embryos (Figs. 8A and 8B) (Ekker *et al.*, 1995; Hammerschmidt *et al.*, 1996a; Macdonald *et al.*, 1995; Ungar and Moon, 1996). Sibling tri^{m209}, kny^{m119}, and kny^{m119} tri^{m209} embryos injected with *shh* (or *twhh*) mRNAs exhibited a generally unchanged mutant morphology (data not shown). Therefore, at the injected doses *hh* mRNA did not rescue or suppress the convergent extension defect in the mutant embryos. Mutant embryos exhibited unilateral or bilateral reduction of retina and pigment epithelium as observed for wild type (Fig. 8; Table 5). Surprisingly, the frequency of

TABLE 4
Morphometric Analysis of Convergent Extension Mutant Embryos

T (°C)	Genotype	AP length 1	AP length 2	wt − *m*Δ	Notochord width	wt − *m*Δ	*dlx3* distance	wt − *m*Δ
23	Wild type	1257 + 43	1295 + 17		47 + 8		359 + 71	
23	*tri*^{m209}	994 + 52	1016 + 41	271	60 + 9	13	485 + 43	126
32	Wild type	1355 + 81	1343 + 88		41 + 8		344 + 44	
32	*tri*^{m209}	1027 + 57	1021 + 58	325	59 + 8	18	415 + 69	71
28.5	Wild type	1381 + 50	1390 + 58		43 + 5		286 + 35	
28.5	*kny*^{m119} A	926 + 109	927 + 107	459	51 + 8	8	416 + 40	130
28.5	Wild type	1459 + 74	1459 + 69		43 + 4		276 + 31	
28.5	*kny*^{m119} B	966 + 100	966 + 65	493	59 + 12	16	411 + 48	135
28.5	Wild type	1403 + 101	1394 + 94		54 + 11		302 + 55	
28.5	*kny*^{m119} *tri*^{m209}	870 + 59	880 + 39	523	96 + 13	42	531 + 47	229

Note. Measurements of embryos at 1 somite stage of development are given in micrometers. Standard deviations represent variations observed in measurements of at least 10 embryos of each genotype. Cyclopia in *tri*^{m209} is enhanced at low temperature (23°C) and suppressed at 32°C. (See Table 2). Anterior–posterior (AP) length of the embryo was determined by measuring from the tip of the head to the end of the tail. AP 1 and AP 2 represent measurements of the same embryo in both lateral views. The width of the notochord was measured at the level of the otic vesicles, and the *dlx3* distance was measured across the neural plate from the otic vesicle on one side to the otic vesicle on the other side of the embryo. wt − *m*Δ represents the difference between wild-type and mutant dimensions.

affected mutant embryos within a clutch was greater than the frequency of affected wild-type embryos (Table 5). Furthermore, *pax6* expression was suppressed in wild-type and mutant embryos injected with *Shh* (*Twhh*) RNA (data not shown). These results indicated that the anterior neuroectoderm of *tri*^{m209}, *kny*^{m119}, and *kny*^{m119} *tri*^{m209} mutant embryos was competent to respond to HH signaling. The eye spacing remained reduced in *tri*^{m209} mutant embryos injected with *hh*, and *kny*^{m119} *tri*^{m209} mutant embryos remained cyclopic (Figs. 8D and 8E and data not shown). Therefore, ectopic HH signaling affected cell fates, but not the abnormal morphogenesis of the eye field in these mutants.

To further explore the potential of the mutants to respond to HH signaling, the expression of the *ptc* gene encoding a candidate receptor for Shh was analyzed (Marigo *et al.*, 1996; Stone *et al.*, 1996). Previous studies have reported a correlation between *ptc1* mRNA accumulation and neuroectodermal and mesodermal cell response to HH signaling in zebrafish embryos (Concordet *et al.*, 1996). At the one-somite stage, *ptc1* RNA was detected in *tri*^{m209} (Fig. 5G), *kny*^{m119} (Fig. 5F), and *kny*^{m119} *tri*^{m209} (Fig. 5H) double-mutant embryos in a domain adjacent to *shh*-expressing cells as described previously for wild-type embryos (Fig. 5E). This provided further evidence that cells adjacent to *hh*-expressing cells could respond to HH signaling. When the expressions of *ptc1* and *dlx3* were analyzed simultaneously, a gap between the anterior edge of *ptc1* and *dlx3* expression domains was observed in *tri*^{m209} (Fig. 5G) and *kny*^{m119} *tri*^{m209} (Fig. 5H) double embryos, but not in wild-type (Fig. 5E) or *kny*^{m119} embryos (Fig. 5F). This indicated that *hh*-expressing cells could activate *ptc1*, a target gene, but not in the anterior-most median position of the neural keel. Taking into account that *ptc1* expression reflects the range of *shh* activity (Chen and Struhl, 1996; Concordet *et al.*, 1996), this observation provides strong support for a failure of the HH signal to reach the anterior region of the neural plate in some *tri*^{m209} and all *kny*^{m119} *tri*^{m209} mutants.

DISCUSSION

Multiple Convergent Extension Genes in Zebrafish Display Overlapping Functions in Eye Morphogenesis

Here we demonstrate that two zebrafish genes, *kny* and *tri*, required for normal convergent extension of the embryonic axis during gastrulation, functionally interact during the specification of the eye anlagen. Three alleles of the *tri* locus, *tri*^{m209} and *tri*^{m747} *tri*^{m778}, resulted in a low frequency of synopthalmic and cyclopic mutants in the AB genetic background. The penetrance and expressivity of the cyclopia phenotype increased in AB/India genetic background. This could be explained by the presence of dominant enhancer(s) of cyclopia in India background or repressors in AB background. *kny*^{m119} mutants only infrequently exhibited synopthalmia in AB/India hybrid background and had normal eye spacing in AB genetic background. However, *kny*^{m119} *tri*^{m209} double mutants exhibited complete cyclopia in AB background. Furthermore, *kny*^{m119} homozygotes with one allele of *tri*^{m209} exhibited an increased cyclopia index, indicating that *tri*^{m209} is an enhancer of cyclopia in *kny*^{m119} mutants.

The *tri* locus has also recently been shown to interact with yet another convergent extension gene, *silberblick* (*slb*) (Heisenberg and Nüsslein-Volhard, 1997). The *tri*^{tc240}

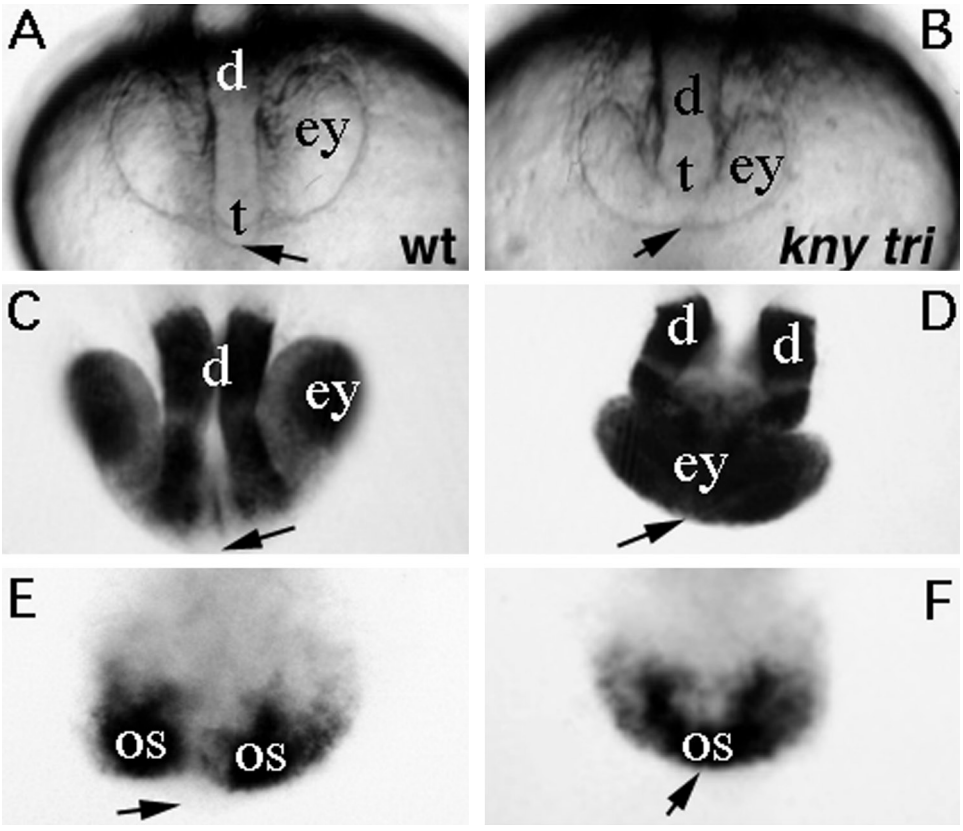

FIG. 7. Abnormal morphology of the optic primordia and ectopic expression of *pax6* and *pax2* genes in the proximal anterior neural plate in kny^{m119} tri^{m209} embryos during the formation of a cyclopic eye. (A, B) Nomarski images of live embryos at the 16-somite stage. In wild-type embryos (A) two separate eye placodes are seen (ey), and the prospective telencephalon (t) and diencephalon (d) are positioned between the eyes at the anterior edge of the neural keel (arrow). In kny^{m119} tri^{m209} mutant embryos (B) one continuous eye placode (ey) is observed with the prospective telencephalon and diencephalon positioned posterior and dorsal to the forming eye. (C, D) *pax6* and (E, F) *pax2* expression visualized by whole-mount *in situ* hybridization. *pax6* expression in wild-type embryos (C) is detected in distal regions of the anterior neural plate in the future diencephalon and eyes and is absent from the median region of the anterior neural plate (arrow). kny^{m119} tri^{m209} double mutants have ectopic *pax6* expression in the median region of the neural keel (arrow), while expression in the prospective diencephalon is compressed and located posterior to the eye field. *pax2* in wild type is expressed in two optic stalks (os) separated by the midline; in contrast, one continuous domain is observed in kny^{m119} tri^{m209} double mutants with ectopic expression in the median region of the anterior neural keel (arrow).

mutant investigated in this work does not manifest cyclopia. However, tri^{tc240} slb^{tx226} double mutants are cyclopic (Heisenberg and Nüsslein-Volhard, 1997). A possible interaction between kny^{m119} and slb^{tx226} as well as between all three loci is currently being investigated by the construction of a kny^{m119} slb^{tx226} tri^{m209} triple mutant line (L.S.K.; Carl-Philipp Heisenberg and Stephen Wilson, Kings College, London, UK, unpublished).

Cyclopia in tri and kny tri Double Mutants Results from Failure to Divide a Single Eye Field

Morphological observations as well as analysis of gene expression patterns indicated that cyclopia in tri^{m209} and kny^{m119} tri^{m209} mutants was a consequence of a failure to properly partition the single optic primordium in the anterior region of the developing neural plate. While in wild-type embryos at the 15-somite stage two distinct retinal primordia separated in the midline by the telencephalon anlage were visible; in kny^{m119} tri^{m209} mutants a single retinal primordium was observed with a bridge of tissue located anterior to the putative telencephalon. This bridge of tissue expressed the *pax6* gene, which was absent from the anterior-most midline position in wild-type embryos. Furthermore, the *pax2* gene expression was reduced and present ectopically in the midline. Similar morphology of the developing eye primordia as well as abnormalities in the expression of *pax6* and *pax2* genes has been reported for *cyc*

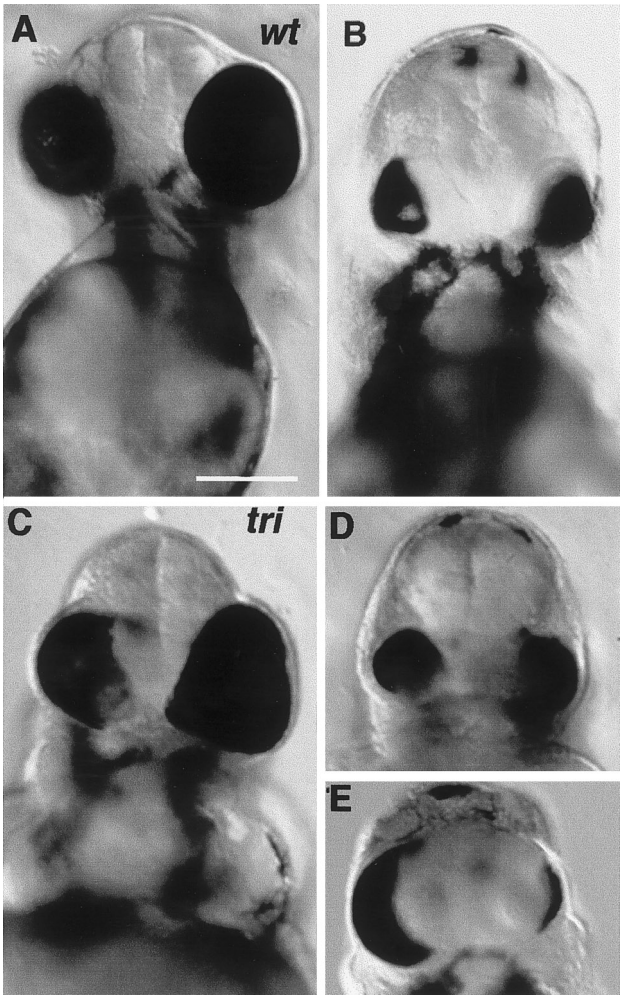

FIG. 8. Effects of *tiggy winkle* (*twhh*) ectopic expression on eye development in wild-type (A, B) and tri^{m209} mutant embryos (C–E) at 48 hpf. *twhh* mRNA (0.1 ng) was injected into zebrafish embryos at the one- to eight-cell stage. In injected wild-type and mutant embryos unilateral or bilateral reduction of retina and pigment epithelium was observed. Notably synopthalmia and cyclopia were still observed in affected mutant embryos (D, E). Bar, 63 μm.

mutants (Ekker *et al.*, 1995; Macdonald *et al.*, 1995) and tri^{tc240} slb^{tx226} double mutants also characterized by cyclopia and convergent extension defects (Heisenberg and Nüsslein-Volhard, 1997). Therefore, the resolution of a single eye field into two separate eyes is dependent on several genes, *tri*, *kny*, and *slb*, whose function is also required for normal convergent extension of the embryonic body. The presence of putative enhancers in India genetic background indicates that the number of these genes is most likely higher. It should be possible to identify such additional genes by simple one-generation enhancer/suppressor screens.

It is noteworthy that the developing eye primordium in kny^{m119} tri^{m209} mutants was smaller at 15 somites than in wild-type siblings. This is in contrast to *cyc* mutants in which the size of the optic primordia at an analogous stage of development does not appear to be significantly affected (Macdonald *et al.*, 1995). Therefore, kny^{m119} tri^{m209} mutants must have patterning or morphogenetic defects in addition to the failure to divide the eye field.

Cyclopia Phenotype in kny^{m119} and tri^{m209} Mutants Is Correlated with the Abnormal Location of Midline Cells, Expressing hh Genes with Respect to the Anterior Neural Plate

The characteristic morphology and the abnormal expression of *pax6* and *pax2* genes are indicative of defects in HH signaling (Ekker *et al.*, 1995; Macdonald *et al.*, 1995). These could result from the absence of HH signals, their abnormal localization in the embryo, or failure of the target tissue to respond to such signals. Based on our studies we propose that in tri^{m209} and kny^{m119} tri^{m209} mutants the defective partitioning of the eye field is a consequence of the abnormal location of *hh*-expressing cells with respect to the developing eye primordium, such that the signal cannot reach appropriate target cells. First, we provided evidence that both *shh* and *twhh* RNAs are expressed in the cyclopic mutants. Second, we demonstrated that tri^{m209}, kny^{m119}, and kny^{m119} tri^{m209} mutants responded to ectopic expression of *twhh* and *shh* RNAs. *pax2* and *ptc* were upregulated in embryos ectopically expressing *hh*, while *pax6* was downregulated, and retina and pigment epithelia were reduced. Furthermore, the mutant embryos expressed *ptc1* RNA in cells neighboring the *shh* expression domain. These observations indicate that tri^{m209}, kny^{m119}, and kny^{m119} tri^{m209} mutants respond normally to HH signaling. Our studies point to abnormal localization of cells expressing *hh* and/or other signals as the primary defect underlying the cyclopia phenotype.

We demonstrated that in the cyclopic mutants the expression domains of the *shh* and *twhh* genes were shortened in the AP dimension at the onset of somitogenesis. Furthermore, a gap was observed between the anterior edge of *shh* (and *twhh*) in the midline and *dlx3* delimiting the anterior edge of the neural plate. Notably, the dimension of the gap correlated with the degree of cyclopia in mutant embryos. We hypothesize that when the dimension of the gap exceeds 40–50 μm, the HH and/or additional signals fail to reach the target tissue resulting in cyclopia.

In imaginal discs of *Drosophila* larvae, HH was shown to have a limited range of action (Chen and Struhl, 1996). It has been proposed that HH limits its own ability to move through tissue by upregulating its receptor, Ptc, in responsive cells. In this model, HH secreted by signaling cells binds to Ptc or the Patched–Smoothened (Ptc Smo) receptor complex expressed at low levels in neighboring cells (Stone *et al.*, 1996). This alleviates the inhibition of Smo signaling

TABLE 5

Effects of Injections of shh and twhh mRNA on Development of Retina and Pigment Epithelium in Wild-Type and Convergent Extension Mutants

	Total number	% surviving at 30 h	Total wt (% affected)	Total *kny* (% affected)	Total *tri* (% affected)	Total *kny tri* (% affected)
Uninjected control	937	91.2	187 (0)	54 (0)	64 (0)	19 (0)
Injected with shh or twhh	1357	86.4	247 (57)	53 (91)	63 (87)	14 (100)

Note. Affected embryos exhibited a reduction of retina and pigment epithelium as previously reported for wild type and cyclops. Interestingly, the percentage of mutants that were affected was greater than wild type. Similar observations were reported for cyclops mutant embryos.

activity by Ptc and results in the upregulation of Ptc expression. High levels of Ptc in response to HH signaling would sequester the diffusing HH, effectively limiting its range of action. Thus, the regions of higher levels of Ptc adjacent to a HH source in the embryo would reveal the limits of HH signaling. It is very likely that the same mechanism limits the ability of vertebrate HH to move through tissue (Concordet and Ingham, 1994). In cyclopic convergent extension mutants, but not in wild type or convergent extension mutants that did not exhibit cyclopia, a gap was observed between the anterior border of the *ptc1* and *dlx3* expression domains. This supports the notion of HH signals not reaching the anterior-most region of the neural plate in cyclopic mutants.

Is the above-hypothesized failure of HH signals to reach target cells the only defect underlying the cyclopia phenotype in tri^{m209} and kny^{m119} tri^{m209} mutants? Abnormally positioned *hh*-expressing cells in the mutants may also be secreting other factors involved in eye field separation. It is conceivable that these factors are also displaced in cyclopic convergent extension mutants; therefore, exposing the anterior neural plate to *hh* alone would not be sufficient to suppress the cyclopia phenotype. Another possibility is that the midline cells may be required to physically separate the eye field. In support of this view, recent fate-mapping experiments indicate that in zebrafish the ventral diencephalic precursors physically invade and thus partition the eye field (Woo and Fraser, 1995; K. Woo and S. Fraser, California Institute of Technology, Pasadena, CA, and Z. Varga and M. Westerfield, University of Oregon, Eugene, OR, personal communication). Therefore, ectopic HH activity would fail to partition the eye field because the midline cells would remain abnormally located and would not separate the eye field in mutant embryos. In tri^{m209} and kny^{m119} tri^{m209} mutants at 24 hpf the anterior compression of the *shh* expression domain indicates that the ventral diencephalon does not form in an appropriate position and therefore could not split the eye field either physically or through a midline-mediated signaling process, resulting in cyclopia. It remains to be determined whether the location of the diencephalon is a consequence of the abnormal location of its precursors at earlier stages of development.

Convergent Extension and Eye Patterning

What causes the abnormal location of the *hh*-expressing cells in cyclopic convergent extension mutants? One possibility is that the location of *shh* and *twhh* expression domains results from abnormal prechordal mesendoderm position with respect to the overlaying neuroectoderm. A convergent extension defect within the prechordal plate could result in its more posterior location. As a consequence, genes activated by the prechordal plate in the overlying neuroectoderm would also occupy a more posterior position. Indeed, at the end of the gastrula stage, the posterior prechordal plate is shorter in the AP axis and broader in the mediolateral direction in tri^{m209} mutants as indicated by the *hlx1* expression pattern (Solnica-Krezel *et al.*, 1996). Here, we demonstrated no positional correlation between *hlx1* and *shh* expression domains at the one-somite stage. A similarly altered shape is observed with Fkd2 expression in the prechordal plate of *slb* mutants (Heisenberg and Nüsslein-Volhard, 1997). Fkd2-expressing cells are not likely to be involved since their location is not correlated with *shh* (Heisenberg and Nüsslein-Volhard, 1997). It is possible that induction by the prechordal plate occurs at an earlier developmental stage such that the position of the prechordal plate and genes activated in the neuroectoderm may not positionally correlate following the onset of morphogenetic movements. Alternatively, a cell population within the prechordal plate other than *hlx1* could be involved. BMP7 in the rat embryo has been shown to cooperate with HH in the prechordal mesoderm to induce ventral midline cell differentiation (Dale *et al.*, 1997). In addition, *cyclops*, a nodal-related gene, has recently been shown to be required for normal prechordal plate development and induction of ventral fates in the CNS (Sampath *et al.*, 1998). One would predict that, like HH, such molecules would be more posteriorly located in cyclopic tri^{m209}, kny^{m119}, and kny^{m119} tri^{m209} mutant embryos.

Another possibility is that the gap between the *hh* and *dlx3* expression domains could result from defective convergent extension movements of ectodermal cells expressing these genes. In this view, the mediolateral narrowing

and AP extension of the *hh* expression domain, driven by the convergent extension movements of the entire population of midline neuroectodermal cells expressing *hh*, contributes to an anteriorward movement of *hh*-expressing cells relative to the surrounding neural plate and consequently to the partitioning of the eye field. As discussed previously, such anteriorward movement of midline cells has been observed in fate-mapping experiments (Woo and Fraser, 1995; K. Woo and S. Fraser, California Institute of Technology, Pasadena, CA, and Z. Varga and M. Westerfield, University of Oregon, Eugene, OR, personal communication). As shown in *Xenopus* embryos, a reduced rate of mediolateral intercalation could lead to altered expression domains for a number of genes (Shih and Keller, 1992). In kny^{m119} and tri^{m209} mutants the *shh* expression domain was not only shorter in the AP direction but also broader in the mediolateral direction. Initial analysis of gastrulation movements in tri^{m209}, kny^{m119}, and kny^{m119} tri^{m209} mutants demonstrated that convergent extension of mesodermal tissues and neuroectoderm was slower in tri^{m209} and kny^{m119} mutants relative to wild-type embryos and dramatically reduced in kny^{m119} tri^{m209} double mutants (L.S.K. and F.M., unpublished observations). slb^{tx226} cells occupy a more posterior position than their wild-type counterparts at 15 hpf. However, no difference in midline neuroectodermal cell migration during gastrulation was detected after transplantation of slb^{tx226} mutant and wild-type cells (Heisenberg and Nüsslein-Volhard, 1997).

It is noteworthy that we observed no simple relationship between the degree of the overall convergent extension defect and cyclopia in tri^{m209} and kny^{m119} mutants. kny^{m119} mutants exhibited a shorter AP axis and *shh* expression domain at the onset of somitogenesis, as well as at 1 dpf, than tri^{m209} mutants. Yet, cyclopia and the *shh*–*dlx3* gap were more prominent in tri^{m209} mutants. We hypothesize that the abnormal location of the *hh* expression domain with respect to the anterior neural plate, and consequently cyclopia, arises when morphogenetic movements of *hh*-expressing cells (or movements of the prechordal plate inducing them) are not coordinated with the morphogenesis of the anterior neuroectoderm. Therefore, the overall convergent extension defect would not lead to cyclopia (e.g., kny^{m119} mutants) as long as the appropriate position of cells expressing *hh* with respect to the anterior edge of the neural plate is maintained. Such failure to coordinate the morphogenetic movements of cells that need to interact during eye development might reflect region-specific requirements for tri^{m209} and kny^{m119} function within the embryo.

ACKNOWLEDGMENTS

We thank Drs. Chuck Kimmel, Alex Schier, Kathy Woo, Chin Chiang, Kimberly Fekany, Encina Gonzalez, Dirk Meyer, Jacek Topczewski, Dina Myers, and the anonymous reviewers for comments on the manuscript and discussions. The kny^{b404} allele was a generous gift from Chuck Kimmel and Charline Walker (Eugene, OR). DNA clones containing the following cDNAs used in this study were kindly provided by our colleagues: *dlx3* (Mark Ekker and Marie-Andree Akimenko, Ottawa, Canada); *hgg1* (Christine and Bernard Thisse, Strassburg, France); *shh* and *pax2* (Stephan Krauss, Umea, Sweden); *twhh* (Stephen Ekker, Minneapolis, MN); and *hlx1* (Anders, Fjose, Norway). This work was supported by NIH RO1 GM55101 to L.S.K., who is a PEW fellow in biomedical sciences.

REFERENCES

Adelmann, H. B. (1936). The problem of cyclopia. Part II. *Q. Rev. Biol.* **11,** 284–304.

Akimenko, M. A., Ekker, M., Wegner, J., Lin, W., and Westerfield, M. (1994). Combinatorial expression of three zebrafish genes related to distal-less: Part of a homeobox gene code for the head. *J. Neurosci.* **14,** 3475–86.

Belloni, E., Muenke, M., Roessler, E., Traverso, G., Siegel-Bartelt, J., Frumkin, A., Mitchell, H. F., Donis-Keller, H., Helms, C., Hing, A. V., Heng, H. H. Q., Koop, B., Martindale, D., Rommens, J. M., Tsui, L.-C., and Scherer, S. W. (1996). Identification of sonic hedgehog as a candidate gene responsible for holoprosencephaly. *Nature Genet.* **14,** 353–356.

Chen, Y., and Struhl, G. (1996). Dual roles for Patched in sequestering and transducing Hedgehog. *Cell* **87,** 553–563.

Chiang, C. (1996). Cyclopia and defective axial patterning in mice lacking sonic hedgehog gene function. *Nature* **383,** 407–413.

Concordet, J. P., Lewis, K. E., Moore, J. W., Goodrich, L. V., Johnson, R. L., Scott, M. P., and Ingham, P. W. (1996). Spatial regulation of a zebrafish patched homologue reflects the roles of sonic hedgehog and protein kinase A in neural tube and somite patterning. *Development* **122,** 2835–2846.

Concordet, J. P., Ingham, P. W. (1995). Developmental biology. Patterning goes sonic. *Nature* **375,** 279–280.

Currie, P. D., and Ingham, P. W. (1996). Induction of a specific muscle cell type by a hedgehog-like protein in zebrafish. *Nature* **382,** 452–455.

Dale, J. K., Vesque, C., Lints, T. J., Sampath, T. K., Furley, A., Dodd, J., and Placzek, M. (1997). Cooperation on BMP7 and SHH in the induction of forebrain ventral midline cells by prechordal mesoderm. *Cell* **90,** 257–269.

Echelard, Y., Epstein, D. J., St-Jacques, B., Shen, L., Mohler, J., McMahon, J. A., and McMahon, A. P. (1993). Sonic hedgehog, a member of a family of putative signaling molecules, is implicated in the regulation of CNS polarity. *Cell* **75,** 1417–1430.

Ekker, S. C., Ungar, A. R., Greenstein, P., von Kessler, D. P., Porter, J. A., Moon, R. T., and Beachy, P. A. (1995). Patterning activities of vertebrate hedgehog proteins in the developing eye and brain. *Curr. Biol.* **5,** 944–955.

Fjose, A., Eiken, H. G., Njolstad, P. R., Molven, A., and Hordvik, I. (1988). A zebrafish engrailed-like homeobox sequence expressed during embryogenesis. *FEBS Lett.* **231,** 355–360.

Fjose, A., Izpisua-Belmonte, J. C., Fromental-Ramain, C., and Duboule, D. (1994). Expression of the zebrafish gene hlx-1 in the

prechordal plate and during CNS development. *Development* **120,** 71–81.

Hammerschmidt, M., Bitgood, M. J., and McMahon, A. P. (1996a). Protein kinase A is a common negative regulator of hedgehog signaling in the vertebrate embryo. *Genes Dev.* **10,** 647–658.

Hammerschmidt, M., Brook, A., and McMahon, A. P. (1997). The world according to hedgehog. *Trends Genet.* **13,** 14–20.

Hammerschmidt, M., Pelegri, F., Mullins, M. C., Kane, D. A., Brand, M., van Eden, F. J. M., Furutani-Seiki, M., Kelsh, R. N., Odenthal, J., Warga, R. M., and Nüsslein-Volhard, C. (1996b). Mutations affecting morphogenesis during gastrulation and tail formation in the zebrafish, *Danio rerio*. *Development* **123,** 143–151.

Hatta, K., Puschel, A. W., and Kimmel, C. B. (1994). Midline signaling in the primordium of the zebrafish anterior central nervous system. *Proc. Natl. Acad. Sci. USA* **91,** 2061–2065.

Heisenberg, C.-P., Brand, M., Jiang, Y.-J., Warga, R. M., Beuchle, D., van Eden, F. J. M., Furutani-Seiki, M., Granato, M., Haffter, P., Hammerschmidt, M., Kane, D. A., Kelsh, R. N., Mullins, M. C., Odenthal, J., and Nüsslein-Volhard, C. (1996). Genes involved in forebrain development in the zebrafish, *Danio rerio*. *Development* **123,** 191–203.

Heisenberg, C.-P., and Nüsslein-Volhard, C. (1997). The function of silberblick in the positioning of the eye anlage in zebrafish embryo. *Dev. Biol.* **184,** 85–94.

Kelly, R., Roessler, E., Hennekam, R., Feldman, G., Kosaki, K., Jones, M., Palumbos, J., and Muenke, M. (1996). Holoprosencephaly in RSH/Smith–Lemli–Opitz syndrome: Does abnormal cholesterol metabolism affect the function of sonic hedgehog? *Am. J. Med. Genet.* **66,** 478–484.

Kessler, D. S., and Melton, D. A. (1994). Vertebrate embryonic induction: Mesodermal and neural patterning. *Science* **266,** 596–604.

Kimmel, C. B., Ballard, W. W., Kimmel, S. R., Ullmann, B., and Schilling, T. F. (1995). Stages of embryonic development of the zebrafish. *Dev. Dyn.* **203,** 253–310.

Krauss, S., Concordet, J. P., and Ingham, P. W. (1993). A functionally conserved homolog of the *Drosophila* segment polarity gene hh is expressed in tissues with polarizing activity in zebrafish embryos. *Cell* **75,** 1431–1444.

Krauss, S., Johansen, T., Korzh, V., and Fjose, A. (1991a). Expression of the zebrafish paired box gene pax[zf-b] during early neurogenesis. *Development* **113,** 1193–1206.

Krauss, S., Johansen, T., Korzh, V., Moens, U., Ericson, J. U., and Fjose, A. (1991b). Zebrafish pax[zf-a]: A paired box-containing gene expressed in the neural tube. *EMBO J.* **10,** 3609–3619.

Lanoue, L., Dehart, D. B., Hinsdale, M. E., Maeda, N., Tint, G. S., and Sulik, K. K. (1997). Limb, genital, CNS, and facial malformations result from gene/environment-induced cholesterol deficiency: Further evidence for a link to sonic hedgehog. *Am. J. Med. Genet.* **73,** 24–31.

Li, H., Tierney, C., Wen, L., Wu, J. Y., and Rao, Y. (1997). A single morphogenetic field gives rise to two retina primordia under the influence of the prechordal plate. *Development* **124,** 603–615.

Macdonald, R., Barh, K. A., Xu, Q., Holder, N., Mikkola, I., and Wilson, S. W. (1995). Midline signalling is required for Pax gene regulation and patterning of the eyes. *Development* **121,** 3267–3278.

Macdonald, R., and Wilson, S. W. (1996). Pax proteins and eye development. *Curr. Opin. Neurobiol.* **6,** 49–56.

Macdonald, R., Xu, Q., Barth, K. A., Mikkola, I., Holder, N., Fjose, A., Krauss, S., and Wilson, S. W. (1994). Regulatory gene expression boundaries demarcate sites of neuronal differentiation in the embryonic zebrafish forebrain. *Neuron* **13,** 1039–1053.

Marigo, V., Davey, R. A., Zuo, Y., Cunningham, J. M., and Tabin, C. J. (1996). Biochemical evidence that Patched is the hedgehog receptor. *Nature* **384,** 176–179.

Riddle, R. D., Johnson, R. L., Laufer, E., and Tabin, C. (1993). Sonic hedgehog mediates the polarizing activity of the ZPA. *Cell* **75,** 1401–1416.

Roelink, H., Augsburger, A., Heemskerk, J., Korzh, V., Norlin, S., Ruiz, i. A. A., Tanabe, Y., Placzek, M., Edlund, T., Jessell, T. M., *et al.* (1994). Floor plate and motor neuron induction by vhh-1, a vertebrate homolog of hedgehog expressed by the notochord. *Cell* **76,** 761–775.

Roessler, E., Belloni, E., Gaudenz, K., Jay, P., Berta, P., Scherer, S. W., Tsui, L.-C., and Muenke, M. (1996). Mutations in the human sonic hedgehog gene cause holoprosencephaly. *Nature Genet.* **14,** 357–360.

Roux, C., Wolf, C., Llirbat, B., Kolf, M., Mulliez, N., Taillemite, J. L., Cormier, V., Le Merrer, M., Chevy, F., and Citadelle, D. (1997). Cholesterol and development. *C. R. Seances Soc. Biol. Fil.* **191,** 113–123.

Saha, M., Servetnick, M., and Grainger, R. (1992). Vertebrate eye development. *Curr. Opin. Genet. Dev.* **2,** 582–588.

Sampath, K., Rubinstein, A. L., Cheng, A. M. S., Liang, J. O., Fekany, K., Solnica-Krezel, L., Korzh, V., Halpern, M. E., and Wright, C. V. E. (1998). Induction of the zebrafish ventral brain and floor plate requires cyclops/nodal signalling. *Nature* **395,** 185–189.

Schier, A. F., Nuehauss, S. C. F., Helde, K. A., Talbot, W. S., and Driever, W. (1997). The one-eyed pinhead gene functions in mesoderm and endoderm formation in zebrafish and interacts with no tail. *Development* **124,** 327–342.

Schmitt, E. A., and Dowling, J. E. (1994). Early eye morphogenesis in the zebrafish, *Brachydanio rerio*. *J. Comp. Neurol.* **344,** 532–542.

Schoenwolf, G. C., and Alvarez, I. S. (1989). Roles of neuroepithelial cell rearrangement and division in shaping of the avian neural plate. *Development* **106,** 427–439.

Schoenwolf, G. C., and Smith, J. L. (1990). Mechanisms of neurulation: Traditional viewpoint and recent advances. *Development* **109,** 243–270.

Shih, J., and Keller, R. (1992). Cell motility driving mediolateral intercalation in explants of *Xenopus laevis*. *Development* **116,** 901–914.

Solnica-Krezel, L., and Driever, W. (1994). Microtubule arrays of the zebrafish yolk cell: Organization and function during epiboly. *Development* **120,** 2443–2455.

Solnica-Krezel, L., Schier, A. F., and Driever, W. (1994). Efficient recovery of ENU-induced mutations from the zebrafish germline. *Genetics* **136,** 1401–1420.

Solnica-Krezel, L., Stemple, D. L., Mountcastle-Shah, E., Rangini, Z., Neuhauss, S. C. F., Malicki, J., Schier, A., Stainier, D. Y. R., Zwartkruis, F., Abdelilah, S., and Driever, W. (1996). Mutations affecting cell fates and cellular rearrangements during gastrulation in zebrafish. *Development* **123,** 67–80.

Stone, D. M., Hynes, M., Armanini, M., Swanson, T. A., Gu, Q., Johnson, R. L., Scott, M. P., Pennica, D., Goddard, A., Phillips, H., Noll, M., Hooper, J. E., de Sauvage, F., and Rosenthal, A.

(1996). The tumor-suppressor gene patched encodes a candidate receptor for sonic hedgehog. *Nature* **384,** 129–134.

Strähle, U., Jesuthasan, S., Blader, P., Garcia-Villalba, P., Hatta, K., and Ingham, P. W. (1997). one-eyed pinhead is required for development of ventral midline of the zebrafish (*Danio rerio*) neural tube. *Genes Funct.* **1,** 131–148.

Thisse, C., Thisse, B., Halpern, M. E., and Postlethwait, J. H. (1994). Goosecoid expression in neurectoderm and mesendoderm is disrupted in zebrafish cyclops gastrulas. *Dev. Biol.* **164,** 420–429.

Ungar, A. R., and Moon, R. T. (1996). Inhibition of protein kinase A phenocopies ectopic expression of hedgehog in the CNS of wild-type and cyclops mutant embryos. *Dev. Biol.* **178,** 186–191.

Westerfield, M. (1996). "The Zebrafish Book." Univ. Oregon Press, Eugene, OR.

Woo, K., and Fraser, S. E. (1995). Order and coherence in the fate map of the zebrafish nervous system. *Development* **121,** 2595–2609.

Received for publication March 10, 1998
Revised July 17, 1998
Accepted July 22, 1998